

Deliverable report for



Sustainable Nanotechnologies

Grant Agreement Number 604305

Deliverable D 7.2
Report on the development of SbyD strategies
applied to WC-Co

Due date of deliverable: 01/04/2016

Actual submission date: 15/06/2016

Lead beneficiary for this deliverable: CONSIGLIO NAZIONALE DELLE RICERCHE – CNR

Authors: Anna Luisa Costa, Magda Blosi, Simona Ortelli, Carlo Baldisserri, Luca Viale

Dissemination Level:		
PU	Public	
PP	Restricted to other programme participants (including the Commission Services)	
RE	Restricted to a group specified by the consortium (including the Commission Services)	
CO	Confidential, only for members of the consortium (including the Commission Services)	X

TABLE OF CONTENTS

1.0 - DESCRIPTION OF TASK 7.2	3
1.1 – STATEMENT	3
1.2 – INTRODUCTION	3
1.3 – METHODS AND PROCEDURES USED FOR WC-Co	4
1.4 – METHODS AND PROCEDURES USED FOR CuO	5
2.0 - DESCRIPTION OF WORK AND MAIN ACHIEVEMENTS	11
2.1 – WC-Co	11
2.1.1 - SPRAY-FREEZE-DRYING GRANULATION	11
2.1.2 – SPRAY-DRYING-GRANULATION	13
2.2– CuO	15
2.2.1 - COLLOIDAL STABILITY: HYDRODYNAMIC DIAMETER AND Z -POTENTIAL	15
2.2.2 - CuO ION RELEASE	18
2.2.3 - THERMOGRAVIMETRIC ANALYSIS ON PRISTINE AND MODIFIED SAMPLES	23
2.2.4 – AGING EVALUATION	25
2.2.5 – XRD AND STEM CHARACTERIZATION	28
3.0 - DEVIATIONS FROM THE WORKPLAN	31
4.0 PERFORMANCE OF THE PARTNERS	32
5.0 CONCLUSIONS	32

1.0 - Description of Task

1.1 – Statement

The work carried out to address Deliverable 7.2 makes reference to activities described in the DoW, under Task 7.1. Title: Report on the development of SbyD strategies applied to WC-Co.

The reverse of two deliverables was agreed at steering board level to focus all the first characterization efforts on CuO in order to share at the same time with other WPs all the information necessary for a sound interpretation of data. For these reasons it impacted in a positive way on the addressing project objectives, as well as on available resources and planning. The present deliverable includes also the data resulting from the extra characterization work performed on pristine and modified CuO, in order to better understand the effects of proposed modifications or of modifications naturally occurring in eco-tox relevant media. The revised and more ambitious objectives addressed for CuO aimed to provide links between basic physicochemical properties and key risk-relevant properties, to improve the knowledge of mechanisms driving any potential adverse effect and to provide useful information for any modeling supporting safer by molecular design approaches. The limited characterization and tests carried out with WC-Co samples were due to less interest gained by this material within SUN consortium that focused collective efforts towards completing and improving CuO physicochemical and biological characterization for getting a fully exhaustive set of data that could be transferred to SUN DSS.

It was agreed with industrial partners to postpone the performance evaluation of modified products, once further information from (eco) tox characterization will be collected and design strategies prioritized. In particular the results of anti-fungal properties on CuO modified samples, and of dustiness tests carried out on pristine and modified WC-Co will be reported in Deliverable 7.7 where general guidelines for risk management of NOAA will be reported, including Safety by Design approach.

1.2 – Introduction

Safer by Molecular Design strategies (SbyMD) are developed with the final goal to produce greener materials with reduced toxicity and associated risks. The main SbyMD strategy proposed for WC-Co is the **micronization** of nanoparticles within nanoscale reactive structures and two kinds of micronization processes are applied: i)spray freeze drying (exploiting freezing and sublimation) and ii)spray drying (exploiting heating and drying). Both micronization processes foresee as first step the powder dispersion in water, exploiting

dispersants to produce stable suspensions, followed by the coupled actions of solvent removal and granulation. A physico-chemical characterization: analysis of morphology (SEM), surface area (BET) and crystalline structure (XRD) is performed on both pristine and modified samples. The granulation is applied as remediation strategy in order to reduce the dustiness behavior of the powder, which will be assessed on the samples before and after modification.

In addition, the results concerning the last advancements of the CuO characterization, not foreseen by the DoW, are presented. In particular, the data involving the complete step by step physico-chemical characterization of pristine and modified CuO nanoparticles when dispersed in media at increasing complexity, from water to biological relevant media.

1.3 – Methods and procedures used for WC-Co

Preparation of WC-Co suspension for spray freeze drying – In a typical preparation 69.3 g of the WC-Co pristine powder was dispersed in 100 ml of water, then 40 g of Duramax D 3021 (solution at 35%wt) was added as dispersant. The so-prepared suspension, labeled as WC-Co_01, has a solid concentration of 41%wt and a concentration of dispersant on the dried powder of 20%wt. The so prepared suspension was ball milled for 2 hours with 5 mm YTZ grinding media.

For the spray freeze drying process, seven samples were prepared by changing the solid content, the amount and the kind of dispersants (table 1). For samples WC-Co_04, 05, 06 and 07 a co-dispersant (binder) was added to the formulations.

Table 1- Formulation of the WC-Co suspensions prepared for the spray freeze drying treatment

Sample	Powder (%wt)	Dispersant (wt%)*	Binder (wt%)*
WC-Co_03_NP_SD_FOR	41	20 Duramax D3021	-
WC-Co_04_NP_SD_FOR	41	20 Duramax D3021	10 PEG 4000
WC-Co_05_NP_SD_FOR	41	20 Duramax D3021	3 PEG 4000
WC-Co_06_NP_SD_FOR	41	-	20 PEG 4000
WC-Co_07_NP_SD_FOR	70	2.3 Duramax 3005	17.6 Duramax B1000
WC-Co_08_NP_SD_FOR	70	1.5 PEG 400	0.5 PEI
WC-Co_09_NP_SD_FOR	70	2 PEG 4000	-

**: the concentration of dispersant is considered as percentage on the dried powder*

- Preparation of WC-Co suspension for spray drying - 100 g of the WC-Co pristine powder was dispersed in 343 ml of water, then 57.14 ml of Duramax D 3005 (solution at 35%wt) was added as dispersant with a concentration with respect to the powder of 20%wt. The so prepared suspension presented a solid loading of 20%wt and it was labeled as WC-Co_10.
- Spray-freeze-drying granulation was performed by using the freeze granulator equipment (LS-2, PowderPro AB, Sweden), nebulizing the suspension directly into liquid nitrogen, so freezing instantaneously the drops which are subsequently lyophilized.
- Spray-drying granulation was performed by using bench-top spray-drier equipment (Spray-dryer SD-05, Lab-Plant Ltd., Huddersfield, England). The suspension was fed at 480 ml/h at a pressure of 1.8 bar and nebulized by means of a 500 μm nozzle in a counter current system with the air at a temperature of 250°C.
- SEM-FEG (Sigma Zeiss, Gemini Column) was used for the morphological characterization of pristine and modified powders. Sol nanoparticles were observed under scanning electron microscopy equipped with a field emission gun (SEM-FEG) and with a transmission electron detector unit (STEM). Images on WC-Co were collected at 3 kV in the reflection mode, while nanoparticles of CuO were observed in the transmission mode at 30 kV. Specimens of CuO for STEM analyses were prepared with a drop of the colloidal suspension, diluted with water (1:100) and deposited on a metallic grid, then evaporated in ambient atmosphere at room temperature.
- BET analysis on pristine and modified powders was performed by applying the BET equation (Thermo Scientific, Surfer) based on the adsorbance of N₂ on the surface of the particles. Before starting the measurement the sample is kept under vacuum and put into a liquid nitrogen bath (-196°C).

1.4 – Methods and procedures used for CuO

Buffer preparation - The selected buffer system for these solutions is the phosphate ion, used to simulate the typical pH of the extracellular fluid (pH = 7.4). The solutions are prepared at a concentration of total phosphate equal to 0.05 M and with a molar ratio (61:39) between the ionic species of HPO_4^{2-} : H_2PO_4^- .

Modifiers agents solutions - A starting solution, 10 ml, is prepared for each modifier agent at a concentration of 0.175 g/mL, in water. Complete dissolution of the modifier agents is reached through mixing and, where necessary, with ultrasonic agitation. Modifier agents considered were:

Na Citrate (CIT), MW 294,10, Aldrich

Polyethylenimine (PEI), MW 750000, Fluka

Na ascorbate (ASC), MW 198,11 Aldrich

PVP (polyvinylpyrrolidone) was not used, because it did not provide satisfactory results as capping agent, as shown by previous analyses.

STOCK and WORKING suspensions: CuO pristine and modified - To prepare 100 mL of CuO STOCK suspensions at a concentration of 10 g/L of Cu (1 wt%): 1.25 g of CuO are placed in a flask prefilled with 50ml of phosphate buffer solution and when occurred the required amount of capping agent (0.125 g, one-tenth of the initial CuO mass) is taken from the correct solution and added; the flask is then filled with buffer phosphate to 100 mL. After homogenization, the suspension is transferred into a 250 mL cylindrical polyethylene flask. 50 mL of 3 mm YTZ grinding media are added in the suspension thus prepared and the cylindrical flask is left stirring on the special rollers, speed 8 for 95 hours. The grinding bodies are separated from each sample.

The following suspensions were so named accordingly with SUN code system:

CuO_101.8_Sol_BM_SYN (pristine)

CuO_102.8_Sol_BM_CIT_SYN (citrate added)

CuO_104.8_Sol_BM_PEI_SYN (PEI added)

CuO_105.8_Sol_BM_ASC_SYN (Ascorbate added)

The digit after the point corresponds to the batch number. During the document the aforementioned samples are sometimes named with shorter labels indicating the progressive number and the kind of modifier.

Working stock suspension are prepared in MILLIQ water at 100 mg/L concentration, starting from FRESH STOCK, CuO_10x_.8_Sol.

Then working stock suspensions were obtained diluting CuO stock suspension, accordingly with concentration used in toxicological tests, in different media: Dulbecco's Phosphate Buffered Saline (D8662), complete DMEM and MEM which consist of commercial biological medium with added 10% v/v Fetal bovine serum (FBS) and 1% v/v Penicillin/Streptomycin (Pen-Strept). It is worthy to note that Dulbecco's Phosphate Buffered Saline (D8662) contains the mixture of salts presents in DMEM and MEM biological media, without aminoacids and proteins, but the

commercial medium, as received, is characterized by a very high saline concentration associated with an high electrical conductivity, thus the working stock suspensions were prepared using diluted (1:10) medium, accordingly with saline concentration in biological media (DMEM and MEM). Media and diluting condition considered in this experiment were 100 mg/L for MilliQ water, D8662 and complete MEM, 50 mg/L for complete DMEM. As regards complete biological media DMEM and MEM, they were left at 37 °C before dilution, otherwise the dilution with Milli Q and D8662 were carried out at room temperature.

Colloidal characterization

The pH was measured both on aged and fresh STOCK samples and on aged and fresh WORKING samples.

Hydrodynamic diameter and the (PSD) by intensity (via dynamic light scattering, DLS) and Z-Potential (via electrophoretic light scattering, ELS) of working stock suspension, diluted in MILLIQ water, were measured with a Zetasizer nano ZSP (model ZEN5600, Malvern Instruments, UK); both particle size distribution and zeta potential analyses were three times repeated and the data provided by averaging these measurements.

Thermal characterization

The thermogravimetric (TG) analyses were carried out at a heating rate of 10 °C/min up to $T^{\circ} = 1000^{\circ} \text{C}$ in air flux by thermo-microbalance (STA 449C, Netzsch-Gerätebau GmbH, Selb/Bavaria, Germany). The analyses were performed on both ultrafiltered and not ultrafiltered samples. Centrifugal filter unit (Amicon Ultra-15, 10 kDa, Millipore) was used to separate adsorbed and free capping agent, allowing to retain capping agent adsorbed on CuO NP surface and filtrate away the free capping agent. Optimal ultrafiltration conditions were obtained with starting volume sample of 15 mL, centrifugal force of 5000 rpm and spin time of 30 minutes. The obtained samples (wet powder, after the elimination of solvent through ultrafiltration) were dried in oven at $T = 100^{\circ} \text{C}$. After the drying, the obtained powders were grinded and analyzed by thermal device.

The following samples were analyzed:

- CuO NP pristine (commercial product)
- CuO_101.6 UF (sample obtained by drying ultrafiltered suspension)
- CuO_101.6 NO UF (sample obtained by drying STOCK suspension)
- CuO_102.6_CIT UF (sample obtained by drying ultrafiltered suspension)
- CuO_102.6_CIT NO UF (sample obtained by drying STOCK suspension)
- CuO_103.6_PVP UF (sample obtained by drying ultrafiltered suspension)

- CuO_103.6_PVP NO UF (sample obtained by drying STOCK suspension)
- CuO_104.6_PEI UF (sample obtained by drying ultrafiltered suspension)
- CuO_104.6_PEI NO UF (sample obtained by drying STOCK suspension)
- CuO_105.6_ASC UF (sample obtained by drying ultrafiltered suspension)
- CuO_105.6_ASC NO UF (sample obtained by drying STOCK suspension)
- Na Citrate (CIT) (commercial product)
- Polyvinylpyrrolidone (PVP) (commercial product)
- Polyethylenimine (PEI) (sample obtained by drying of commercial solution 50 wt% in water)
- Na ascorbate (ASC) (commercial product)
- Na Phosphate monobasic dihydrate (PHOSPH) (commercial product)

Release of ions

Ion release was estimated by evaluating the Cu^{2+} ionic copper to total copper oxide ratio. In order to calculate the ratio ($\text{Cu}^{2+}/\text{CuO}$ %), 15 mL of working stock suspensions were centrifuged using Ultra-Centrifugal Filter (UCF) unit (Amicon Ultra-15, 10 kDa, Millipore), centrifugal force of 5000 rpm and spin time of 30 min. The UCF unit allows retaining CuO NPs and filtrating away the Cu^{2+} ions, this way 10 mL of filtered solvent, which contains the dissolved Cu^{2+} were subjected to elemental analysis using Inductively Coupled Plasma - Optical Emission Spectrometry (ICP-OES). In order to assess the total copper amount contained in the working stock suspensions, ICP analysis were performed also on the complete working stock, which was properly treated with 2 mL of ultrapure HNO_3 (99.99%) and (...) previous to be analyzed.

Electroanalytical method for the ion release measurement

CuCl₂ solution Stock Cu(II) chloride (CuCl_2) solutions (1.67 mol L^{-1}), to be used to add known amounts of Cu^{2+} ions to PBSBs, DMEM or FBS-DMEM for calibration purposes, were prepared by direct reaction of stoichiometric amounts of CuO nanopowder and HCl (Sigma-Aldrich 2258148, Lot # SZBD1160V, 37% assay (36.5÷38.0)). Part of the stock Cu(II) chloride solution was further diluted with Millipore water to obtain a suitable concentration ($12 \text{ } \mu\text{mol mL}^{-1}$) of Cu^{2+} ions to be added to the media.

Aqueous glycine solution Glycine solution was prepared shortly before use by dissolving 0.962 g of glycine (Aldrich SIGMA-Life Science, ReagentPlus®. ≥ 99%, G7126, Lot# SZBB0690V) in Millipore water, topping the volume at 10 ml (final glycine concentration: 1.286 mol L^{-1}).

Au working electrode Au was chosen instead of Ag to rule out the possibility of Ag oxidation and AgCl formation in chloride-containing media. The Au working electrode (WE) was built using 10 cm of gold wire (Goodfellow, 99.99% purity, 100 μm diam.) inserted into a Pasteur pipette, of which 14 mm protruded out of the thin end of the pipette. We made no attempts to make an Au/glass seal by melting the tip of the glass tube onto the gold wire, since it has been reported in the literature that this type of joint is not very reliable as to impermeability. Instead, we chose to melt a pearl of polyethylene at the tip of the glass sleeve, so that a good seal would form at low temperature (about 200°C) between Au, polyethylene, and glass. Microscopic inspection showed that a faultless joint had been formed, due to wetting of both glass and Au by molten polyethylene. To avoid complications involved in making soldered contacts or using conductive epoxy, the electric contact to the working electrode input of the potentiostat was made directly on the gold wire at the other end of the pipette. The projected area of the Au working electrode was $4.4 \times 10^{-3} \text{ cm}^2$.

Counter electrode The counter electrode (CE) was a coiled length (10 cm) of 0.5 mm diam. platinum wire (Goodfellow, 99.99% purity) that was sealed in a Pasteur pipette in a similar way to the WE using epoxy resin. The area of counter electrode in contact with the solution was 1.5 cm^2 , i.e. about 340 times the projected area of the WE. The electric contact to the CE input of the potentiostat was made by soldering one end of the Pt wire to a length of wire-wrap silver-coated copper wire. The joint was encased in epoxy resin for electric and chemical insulation purposes.

Reference electrode and salt bridge The reference electrode (RE) was a saturated calomel electrode (SCE, type 303/SCG/12 from AMEL srl, Milan, Italy) that during the measurements was kept in a separate polyethylene container filled with 3M potassium chloride (Sigma Life Science Potassium Chloride P5405, Lot # SLBC3868V). The potential of this SCE is +0.2444 V vs. standard hydrogen electrode (SHE). The SCE was put in electric contact with the solution in the cell through a 3% agar-agar/3M KCl salt bridge in polyethylene tubing (E-406, food grade Agar Agar, B&V srl, Italy, total metals content < 10 ppm). One end of the salt bridge was dipped in the solution that filled the Luggin capillary, the tip of which was placed in proximity of the working electrode. Given the good conductivity of all solutions, however, potential shifts due to the cell's IR drop were a minor concern.

Electrochemical cell The three-electrode electrochemical cell was set up using a three-neck round-bottom borosilicate glass flask with a central 29/32 and two lateral 14/23 conically tapered ground joints. Holes were drilled in matching standard plastic stoppers to house the glass shaft of the WE, CE and Luggin capillary. The inner cone of the stoppers was then filled with epoxy resin to block the shafts relative to the body of the stoppers. The spatial

arrangement of the three electrodes was set by introduction and axial rotation of the stoppers in the ground joints. The distance between the Au WE and the tip of the Luggin capillary was about 3 mm, that between WE and CE about 30 mm. The volume of the solution in the cell was 120 ml.

Electrochemical workstation The electrochemical workstation was a Metrohm μ AutoLab FRA2 – Type III unit (Eco Chemie, the Netherlands) having ± 5 V compliance voltage, 80 mA maximum current, 10 nA minimum current range and $\pm 0.2\%$ current resolution. The Nova 1.6 proprietary software was employed to design and control the experiments, and for data processing and displaying. Recorded electrochemical data were saved in .txt format for easy processing in other software platforms, such as Microsoft Excel or NI LabView.

General laboratory practice Glassware was cleaned by a 30 min. immersion first in a saturated solution of potassium hydroxide in ethanol and then in 1 M HCl, followed by profuse rinsing in tap and distilled water. Preliminary steps to the measurements included thorough washing of the glassware and electrodes, first with distilled and then with 18.2 M Ω cm Millipore water. In order to eliminate organic contaminants, the Au working electrode was cleaned by alternate dips in concentrated H₂SO₄ (Carlo Erba Sulfuric Acid, Min. Assay 96% ISO-For Analysis, Code No. 410301, Batch Number 4L1751858) and 35% hydrogen peroxide (Aldrich, Hydrogen Peroxide 35 wt% solution in water, Cat. 34988-7, Lot S23803-294), a procedure described in the technical literature as *in situ* piranha cleaning (see: *Procedure on handling and using Acid Piranha Solution*, University of Cambridge's Department of Chemistry, Technical Note), followed by rinsing in Millipore water. In order to obtain reproducible quantitative results, a procedure for checking - and possibly reproducing - the active area of the Au electrode had to be employed. Cyclic voltammetry (CV) scans in 1 mol L⁻¹ H₂SO₄ were used to check the electrode for standard electrochemical behavior and active area, as described below. All CV experiments were performed at room temperature ((20 \pm 1)°C).

2.0 - Description of work and main achievements

2.1 – WC-Co

Spray granulation techniques have been successfully applied in the Sanowork project to agglomerate/aggregate powders and control their aerosolization during manufacturing steps such as powder recovery, handling, weighing, stocking or drying. They have been proposed as “nano in micro” design options and evaluated in terms of reduced dustiness and preserved or improved properties. The same approaches have been re-proposed in the SUN project and in particular for the WC-Co samples

WC-Co pristine powder is provided by MBN nanomaterialia and fully characterized in deliverable 1.4.

2.1.1 - Spray-freeze-drying granulation

Some of the most promising suspensions were analyzed by means of sedimentation tests as shown by the images (fig. 1). All the samples evidenced a precipitate during the 24 hours, but the sample WC-Co_03 showed the best stability in terms of sedimentation rate, while the samples WC-Co_04 evidenced a rapid phase separation between the dispersant and the binder with the subsequent solid precipitation

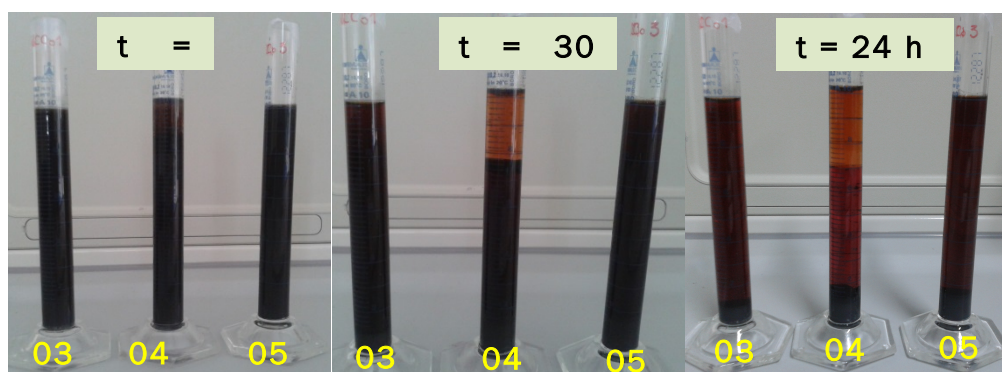


Fig 1 – Sedimentation tests on samples WC-Co 01, 02, 03.

The spray-freeze-granulation was performed on all the prepared samples. Figure 2 showed the SEM analyses of some of the WC-Co samples before (Fig 2a) and after (Fig. 2b, c, d, e) the freeze-granulation treatment. After granulation the particles are not regular and spherical as expected, but most samples (WC-Co06_ FD, WC-Co08_FD, WC_Co09_FD) evidenced the same irregular appearance of the pristine powder. In these cases the granulation was not achieved probably due to the high precipitation tendency of this powder, which causes a separation in the just formed drop, avoiding the homogenous freezing.

Instead, sample WC-Co03 (Fig 2b), corresponding to the best dispersed sample, showed spherical micrometric particles, but very rare and isolated. In this case the granulation occurred, but only partially, always due to the high density of the powder which induces phase separation within the freezing drops.

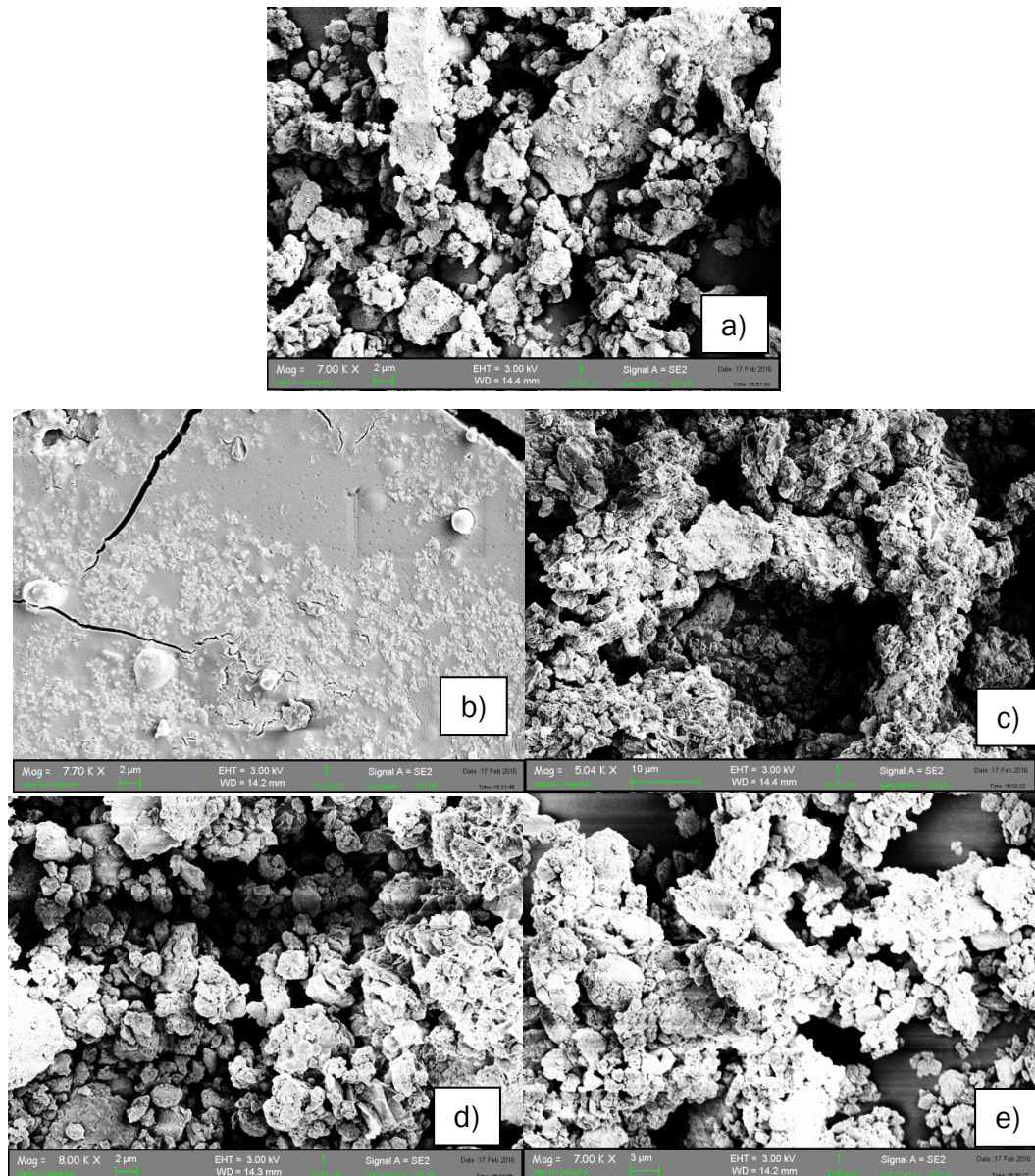


Fig 2 – SEM images of: WC-Co pristine (a), WC-Co03_FD (b), WC-Co06_FD (c), WC-Co08_FD (d), WC-Co09_FD (e)

2.1.2 – Spray-drying-granulation

The aqueous suspension WC-Co_10 was granulated by means of the spray drying process and named WC-Co_10_NP_SD_FOR. This way the granulation was performed exploiting the sudden drying of the drop exposed to a hot air current (250 °C). The fast solvent evaporation prevents the phase separation inside the drops, promoting the formation of the spherical shape as proved by the SEM images (Fig 3).

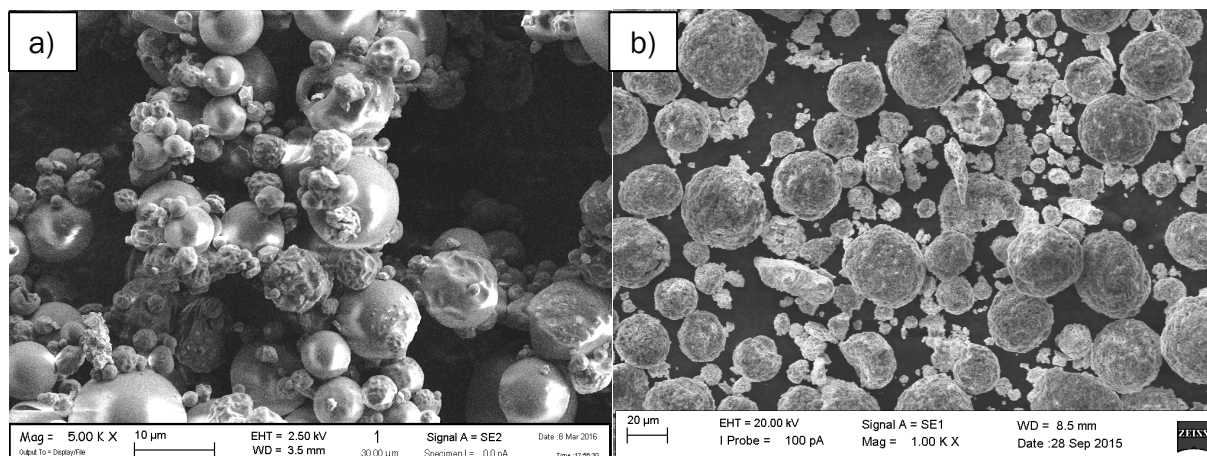


Fig 3 – SEM images of a) sample WCCo_10 after spray drying at different magnification and comparison with spray-dried sample commercialized by MBN, c).

The morphology of sample WC-Co_10_ NP_SD_FOR was compared with that of commercial sample spray-dried by partner MBN (WC-Co_2_ NP_SD_FOR) starting from organic solvent dispersion of the same pristine powder and deposited as a thick, wear resistant coating by Thermal Spraying (see Deliverable 3.1 for details). This type of coating is used on the rolls in the paper and textile industries and in the blades used for industrial paper scrapping.

The advantage of having granulated powder stems in the control of the dustiness behavior but maintaining a great surface area and reactivity. In line with expectation the so granulated powder, showed higher specific surface area (16.88 m²/g), if compared with pristine powder, probably due to the good dispersion grade achieved during the suspension preparation. The commercial (WC-Co_2) and new spray-dried (WC-Co_10) powders will be compared as far as their dustiness behavior is concerned in order to see if the new proposed process of dispersion in water and spray-drying could promote the formation of more dense and compact granules as SEM observation could suggest. The NRCWE partner will performed dustiness tests and the results reported in deliverable 7.7, where within guidelines for the implementation of risk management measures the safety-by-product-design approach developed for CuO and WC-Co materials will be discussed and evaluated.

Table 2 – SSA of the pristine and modified WC-Co powders

Sample	SSA (m ² /g)
WC-Co_01 (pristine)	1.41
WC-Co_10_SD	16.88

XRD analysis performed on the granulated powder confirmed that the spray drying process did not modify the crystalline phase, which was confirmed as tungsten carbide (100%).

2.2– CuO

2.2.1 - Colloidal stability: hydrodynamic diameter and ζ -potential

Pristine and modified CuO materials were widely characterized in terms of key determinant properties: colloidal stability, surface charge and ions release (Cu^{2+}/Cu ratio) in relevant biological media (MEM and DMEM). The modifying agents, fully described in the deliverable 7.1, differ for their charge: positive charged polyethylenimine (PEI), negatively charged citrate (CIT), ascorbate (ASC) and neutral polyvinylpyrrolidone (PVP).

Table 3 – Summary of the modified CuO samples.

Sample code	Description	Charge fo the modifiers
CuO_101_Sol_BM_SYN	Pristine	
CuO_102_Sol_BM_CIT_SYN	Modified with Citrate	Negative
CuO_103_Sol_BM_PVP_SYN	Modified with PVP	Neutral
CuO_104_Sol_BM_PEI_SYN	Modified with PEI	Positive
CuO_105_Sol_BM_ASC_SYN	Modified with Ascorbate	Negative

A step by step characterization was applied to follow the evolution of both pristine and modified NP properties at increasing medium complexity (from distilled water to biological fluids) and to understand how they are affected by the surrounding matrix components (pH, ionic species, biomolecules) (Fig 4).

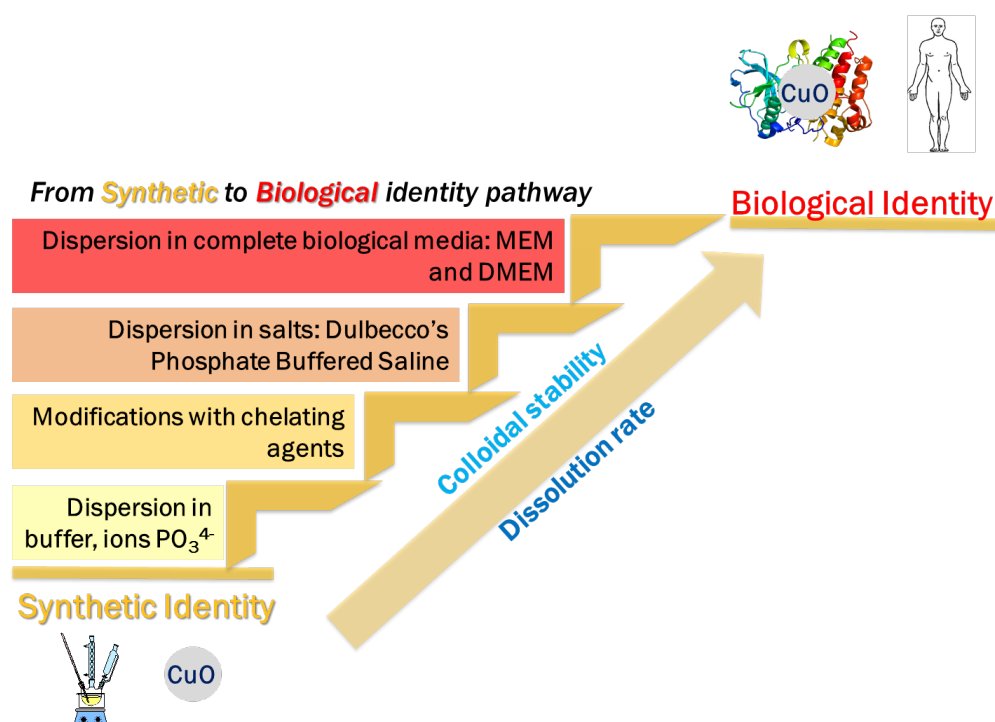


Fig 4 – Scheme of the step by step characterization in medium with increased complexity

Colloidal stability (through hydrodynamic diameter and ζ -pot measurements) is one of the NP key descriptors considered because it influences most of the other properties, and thus has a great influence on toxic outcomes. In particular the effect of modifying agents on CuO NPs potential for agglomeration was assessed, because a colloidal stabilization by electrostatic (CIT, PEI and ASC) or steric (PVP) repulsion forces was expected. DLS results, referred to pristine and modified CuO NPs diluted in buffered MilliQ water, DMEM and MEM, are reported in Table 4.

Table 4. Size data (d_{DLS}) of pristine and modified CuO samples dispersed in different media: MilliQ water, D8662, DMEM and MEM.

Sample	d_{DLS} (nm)			
	MilliQ	D8662	DMEM	MEM
CuO_101	1093 \pm 50	2756 \pm 347	55 \pm 16	47 \pm 6
CuO_102_CIT	368 \pm 10	271 \pm 43	37 \pm 2	89 \pm 5
CuO_103_PVP	797 \pm 84	2765 \pm 432	53 \pm 25	44 \pm 2
CuO_104_PEI	247 \pm 14	209 \pm 16	45 \pm 14	46 \pm 4
CuO_105_ASC	122 \pm 1.4	1314 \pm 525	73 \pm 21	52 \pm 4

d_{DLS} (nm) DMEM and MEM = 17 \pm 0.3 and 21 \pm 0.5, respectively

The data in MilliQ confirmed the expected effect of surface modifiers addition. In fact, samples coated by ionic agents (negative CIT and ASC, positive PEI) resulted better dispersed with a significant decreasing of average hydrodynamic diameter size in comparison with pristine sample. On the other hand, neutral PVP did not improve significantly the dispersion of CuO NPs, probably the long organic chains forced nanoparticles aggregation by depletion flocculation phenomenon [1]. Data collected in D8662 showed an increase of hydrodynamic diameter, if compared with the results in MilliQ water. This is correlated to aggregation phenomena and justified by the increase of ionic strength due to the salts content in Dulbecco's Phosphate Buffered Saline (D8662) medium. Salts screen charge on the NP surface reducing electrostatic repulsion [2]. Otherwise, negative CIT and positive PEI modified samples have a hydrodynamic diameter compared with that in MilliQ water. In particular, PEI modified resulted the best disperse. A possible explanation could stay in the electrosteric action of polyethylemmine [3]. Ascorbate and citrate salt can only improve the repulsive potential due to the negative charge transferred to particle surface. PEI provides both electrostatic contribute due to positive charge and steric action due to polymer structure, so for this reason PEI coated samples result stabilized also in high ionic strength medium (D8662).

Data collected by samples diluted in cell culture media DMEM and MEM are not particularly significant in terms of DLS mean diameter. The results are comparable with values of DMEM and MEM (17 and 21 nm, respectively), obtained analyzing pure cell culture media with DLS technique.

ζ-potential greatly affects both the colloidal stability and the interaction of NPs with the biological environment [4,5]. Basically, the charge is often quantified in terms of ζ-potential which depends on the medium in which the NPs are dispersed and, therefore, it is strongly correlated to the pH [6]. The results collected for the CuO samples are listed in Table 6.

Table 5. ζ-potential (ζ-pot_{ELS}) of pristine and modified CuO samples dispersed in different media: MilliQ water, D8662, DMEM and MEM.

Sample	ζ-pot _{ELS} (mV)				pH			
	MilliQ	D8662	DMEM	MEM	MilliQ	D8662	DMEM	MEM
CuO_101	-9.1 ± 0.4	-2.3 ± 2.1	-8.2 ± 0.4	-10.1 ± 0.5	6.5	7.5	8.0	8.2
CuO_102_CIT	-18.0 ± 0.3	-3.4 ± 1.2	-9.7 ± 0.6	-10.5 ± 0.2	6.5	7.4	7.9	8.2
CuO_103_PVP	-8.1 ± 2.3	-0.9 ± 0.7	-9.4 ± 0.8	-10.1 ± 0.4	6.5	7.4	7.9	8.2
CuO_104_PEI	+28.3 ± 0.7	+13.8 ± 0.1	-10.1 ± 0.7	-10.5 ± 0.9	6.5	7.4	7.9	8.2
CuO_105_ASC	-17.4 ± 0.3	-8.1 ± 0.1	-9.2 ± 0.2	-9.5 ± 0.2	6.4	7.4	7.9	8.2

ζ-pot_{ELS} and pH of DMEM = -10.6 ± 0.3 mV and 7.9; ζ-pot_{ELS} and pH of MEM = -9.9 ± 0.2 mV and 7.9

Pristine CuO NPs diluted in MilliQ water (CuO_101), showed a negative zeta potential, despite to the expected positive value of copper oxide and in general of basic metal oxides when dispersed in water [7]. This is justified by the presence in the stock dispersion of phosphate ions (PO₄³⁻), which are specifically adsorbed onto CuO NPs surface, transferring the negative charge. This suggests that the formation of negative NP complex in biological environmental (phosphate buffer) occurs independently of aminoacids and proteins. The key role of phosphate adsorption [8] is, here, demonstrated by the reversal of surface charge sign, whereas other indifferent ions can only screen the surface charge, as shown by ζ-pot data in D8662. The modified samples diluted in MilliQ water showed values coherent with the charge given by the modifier agents, confirming the preferred interaction of aforementioned modifiers over phosphate ions. As expected, the addition of neutral PVP coating did not modify the ζ-potential of pristine sample. In D8662, the increase of ionic strength induced a colloidal destabilization, as confirmed both by the increased agglomeration degree (Table 5) and by ζ-

pot decrease (Table 6). The found coherence between NP size and ζ -pot results confirmed that DLS coupled with ELS represent an effective tool for the colloidal stability evaluation. When aminoacids and protein are added in the media, as for complete DMEM and MEM, ζ -pot data are levelled off on the typical value of the biological medium alone (negative ζ -pot around -10 mV, see Table) because, according to protein corona theory, NPs are covered by proteins immediately upon contact with a biological environment. Moreover, the results obtained by the samples dispersed in complete DMEM and MEM showed that the interaction between the CuO NPs and the biomolecules overwhelmed the effects of surface-modifying agents, otherwise phosphate ions has a secondary role in biophysical adsorption, as revealed by ζ -pot data in the absence of modifying agents or proteins. In particular, the proteins of serum (FBS) have a key role being primarily involved in protein corona formation and nano-bio interactions, as many papers report

2.2.2 - CuO ion release

Ultrafiltration and ICP analysis

Ions release was estimated by evaluating the Cu^{2+} ionic copper to total copper oxide ratio, the results were obtained after ICP-OES on filtrates of ultra-centrifuged working stock suspensions.

Table 6. $\text{Cu}^{2+}/\text{CuO}$ weight ratio % of pristine and modified CuO samples dispersed in different media: MilliQ water, D8662, DMEM and MEM.

Sample	$\text{Cu}^{2+}/\text{CuO}$ (%)						
	MilliQ		D8662	DMEM		MEM	
	t = 1h T 37 °C	t = 24h T 37 °C	t = 95h room T	t = 1h T 37 °C	t = 24h T 37 °C	t = 1h T 37 °C	t = 24h T 37 °C
CuO_101	0.34	0.18	<0.31	53.53	67.41	49.79	59.91
CuO_102_CIT	1.85	1.98	1.81	53.77	69.19	37.11	55.22
CuO_103_PVP	0.79	0.23	<0.33	56.80	66.93	40.52	34.00
CuO_104_PEI	1.68	2.84	2.55	49.58	66.01	27.99	43.06
CuO_105_ASC	2.08	1.99	<0.33	50.51	65.39	34.31	48.13

As can be observed by data collected in DMEM and MEM the dissolution dramatically increased in biological environment, reaching after 1 hour, for DMEM, values of the Cu^{2+}/Cu ratio ranging from about 50 to 56% and attaining the 69% after 24 hours. For MEM the data showed slightly lower values at 1 hour, reaching dissolution grades from 34 till 59% after 24 hours. Being pH of Eagle's media buffered around 8, a possible explanation of the dissolution

enhancement can be the chelating effect of aminoacids and proteins which subtract Cu^{2+} ions from the dissolution equilibrium. The increased dissolution/release of Cu^{2+} from CuO NPs suspended in biological media compared to samples dispersed in MilliQ and D8662 (Phosphate Buffered Saline medium) have been shown by other studies [9]. The general low solubility found in D8662 (dissolution below 3%) further confirmed the primary role of protein components that promote dissolution. Considering only the medium without aminoacids and proteins (MilliQ and D8662), it is observed that the highest values were found in citrate and PEI modified samples. This confirms that the degree of particle solubility and dissolution depends on the particle characteristics as well as on the properties of the medium, as exposure environmental, unless the features of the medium not prevail over the complete system [10]. Furthermore, in support to this, a size dependent solubility is shown in the samples dispersed in MilliQ and D8662. At low aggregation degree correspond a high solubility (CuO_102 _CIT and CuO_104_PEI, CuO_105_ASC). Otherwise, the samples resulted more aggregated (CuO_101, CuO_103_PVP) showed very low values of Cu^{2+} /CuO weight ratio (%).

Electroanalytical methods

Ion release was usually assessed exploiting ultrafiltration to separate the ionic fraction followed by the ICP elemental analysis on the extracted solvent. Although this method is highly reliable it presents some drawbacks in fact it is disruptive and time consuming. In order to overcome these problems an electroanalytical method, exploiting a three electrode system, has been developed, allowing the detection of Cu^{2+} in a CuO aqueous suspension, this way Cu^{2+} ions can be revealed in situ even in biological media. Electroanalysis at the Au electrode has been employed to detect and quantify copper ion leaching in various biological media (Aldrich D8662 and D4031 phosphate buffered phosphate buffers (PBSBs), Dulbecco's Modified Eagle's Medium (DMEM), and fetal bovine serum-added DMEM (FBS-DMEM)). In order to do so, calibration curves of Cu^{2+} in all media were obtained by correlating the known nominal concentration of Cu with the height of anodic peaks appearing during cyclic voltammetry (CV) scans. Cu^{2+} ions were added to the media as copper chloride (CuCl_2) solution, up to 200 μmol nominal Cu^{2+} concentrations. Anodic peaks were observed, and interpreted as due to stripping of Cu deposited onto the Au electrode during a previous cathodic run. The position E_{PEAK} of the peak on the potential axis, and its height I_{MAX} , were recorded and plotted vs. nominal Cu^{2+} concentration (Fig. 5). Monotonically increasing and reproducible peak height vs. $[\text{Cu}^{2+}]$ calibration curves could thus be obtained in Aldrich D4031, DMEM and FBS-DMEM. As to Aldrich D8662, no reproducible correlations between Cu concentration and peak height could be observed.

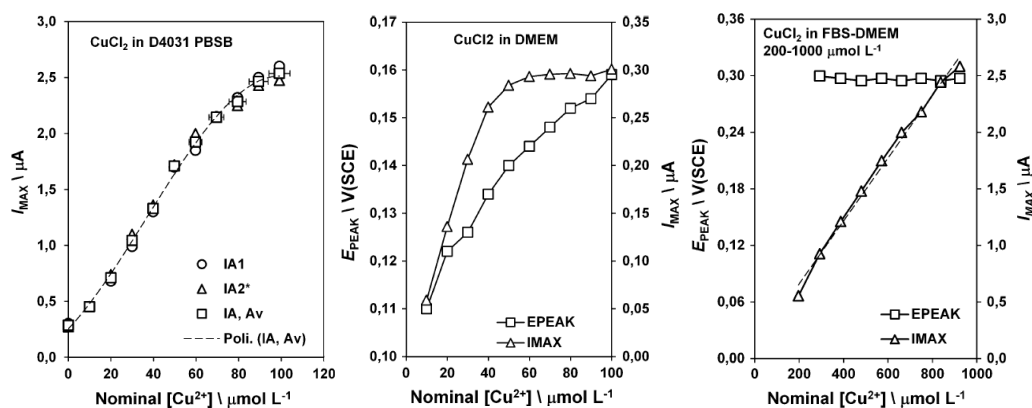


Fig. 5 Calibration curves for Cu in D4031 PBSB (left), DMEM (center), FBS-DMEM (right) [13]

The same deposition/stripping CV scans were then performed in the same media (but Aldrich D8662) to which copper(II) oxide (CuO) nanoparticles (NPs) had been added. NPs were added to the media as aqueous suspension (11% v/v of 1 g L⁻¹ CuO in DI water). The same anodic peaks appeared as those observed in CuCl₂-added media (Fig. 6).

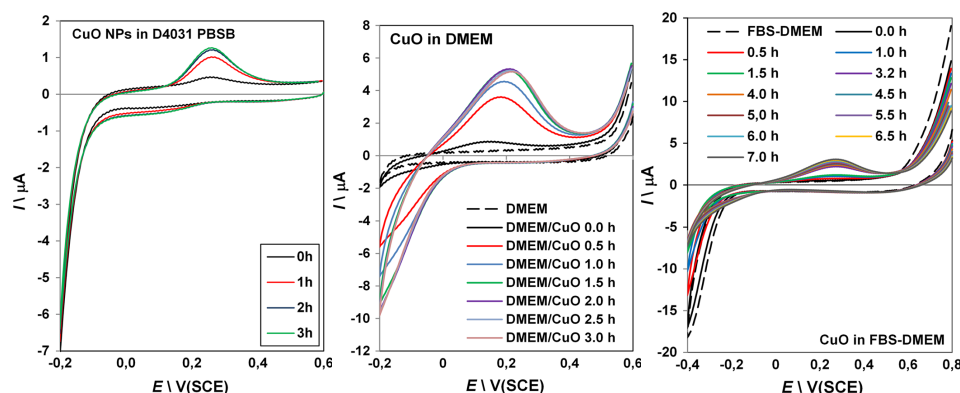


Fig. 6 - CV curves recorded in CuO-added D4031 PBSB, DMEM, and FBS-DMEM. The height of the anodic peak was observed to increase vs. time. CV curves recorded in CuCl₂-added media were similar [13].

While all the above provides strong evidence of copper leaching in suspensions of CuO NPs in biological media at pH 7.4, minor differences were observed in the electrochemical response of the CuO-NPs-added media with respect to that observed in CuCl₂-added media. The effect of adding glycine to CuCl₂-added D4013 PBSB was also studied, providing evidence that minor differences in the electrochemical behavior of Cu in DMEM and FBS-DMEM - as compared to D4031 PBSB - could be explained by the presence of the amino acids present in DMEM and FBS-DMEM. Electroanalysis results thus far obtained strongly indicate that Cu leaching from CuO NPs is to be expected as a matter of course both in CuO NPs aqueous suspensions and suspensions in biological media, from a few percent of the total copper content in D4031 PBSB to 80% in FBS-DMEM over a few hours. Electroanalysis has been found to be helpful in

monitoring and describing the chemical environment determined by the presence of CuO-NPs in the above media. In particular, Cu leaching has been observed at pH 7.4, questioning the stability of CuO NPs in buffered biological media. In the case of CuCl₂ in D8662 PBSB, electroanalysis provided strong evidence of some chemical mechanisms that were able to either subtract copper or inactivate it electrochemically, so that increasing amounts of added copper did not cause stronger CV copper features to be observed. The possible role of phosphate ions in this mechanism is currently being studied by means of CV at the platinum electrode. The trend of anodic features vs. time can be utilized to infer the kinetics of the leaching mechanism. In conclusion, electroanalysis (an in situ, noninvasive and easily implemented technique) has evidenced both presence of Cu ions in the above media to which CuO NPs had been added, and the presence of mechanisms that seem to be able to electrochemically inactivate ionic copper. Such mechanisms seem to involve the role of phosphate ions, amino acids, and perhaps glucose, as evidenced by the comparison between results of CuCl₂ in D8662 PBSB and D4031 PBSB (Fig. 7).

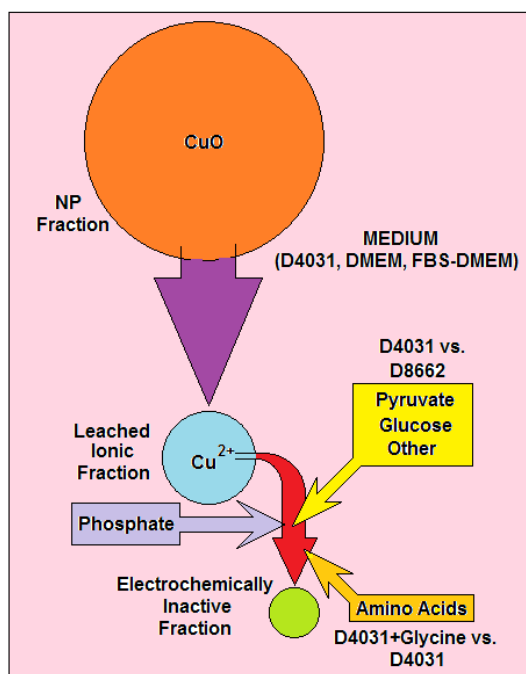


Fig. 7 - Schematic of the overall picture so far contributed by electroanalytical measurements to the mechanisms operating in CuO NPs-added biological media. Two main mechanisms are envisaged: Cu leaching, and inactivation of leached Cu²⁺. The latter seems to be dependent on the presence or absence of medium components such as glucose, pyruvate, amino acids, and phosphate ions.

Electroanalytical experimental activity was carried out starting in October 2015, and is still being pursued. Number of electrochemical experiments so far performed is in the range of a few hundreds, including experiments that did not furnish conclusive results. An extensive

literature review was undertaken before starting the activity, which made it clear that CuO-added biological media were extremely complex systems, both from a chemical and an electrochemical standpoint. As far as we know, there was a single instance in the literature reporting similar experiments, although dealing with Ag rather than Cu ions in biological media. Accordingly, the first part of the activity was explorative rather than quantitative. Results obtained were possible due to the anodic stripping peaks used for electroanalysis appearing in the double-layer region of all pristine media investigated. This circumstance afforded a good resolution of the anodic features of copper, and a good Cu signal-to-noise ratio, starting at concentrations of Cu about $10 \mu\text{mol L}^{-1}$. Lower concentrations may be quantitatively determined using microelectrodes, but the amount of leached copper is usually large enough to allow quantitative electrochemistry using conventional electrodes. An Au microelectrode has anyway been prepared, and is available should quantitative electrochemistry of smaller Cu concentrations in biological media be needed.

The activity has involved the design of suitable electrochemical protocols and their practical implementation, the latter including the construction of several working electrodes, their preparation and characterization in standard acidic solutions, and the selection of the best performing electrodes. Working electrode materials investigated included Au, Ag, Pt, and LPE (lead pencil electrode). The activity has included the selection, acquisition and set-up of an Autolab PGSTAT 302N electrochemical workstation, whose purchase was considered after results obtained on a smaller Autolab unit - whose use was granted for free by the owner (University of Bologna) - indicated that the amount of information to be extracted by means of electrochemical techniques was a valuable addition to that from techniques already available to the Research Group.

Part of the results so far obtained may provide better insight on issues as CuO NPs stability, extent of copper leaching and chemical processes taking place in CuO-added biological media. Detailed information on methods and results can be found in the published work. The balance between NP-related cytotoxicity and ion-related cytotoxicity in copper-containing biological media may be better understood based on such findings.

2.2.3 - Thermogravimetric analysis on pristine and modified samples

The evaluation of the capping agent amount adsorbed on CuO NP surface was performed by thermal analysis on the dried CuO modified samples. In order to distinguish the adsorbed capping agent from the free one, the free capping was eliminated by ultrafiltration of the STOCK suspensions (10 g/L) and the adsorbed agent quantified by thermogravimetric analysis on the dried CuO powders. The weight loss percentage of the ultrafiltered (UF) and not ultrafiltered (NO UF) modified samples were compared and normalized with respect to the pristine sample loss (CuO NP pristine) and to the phosphate coated sample loss (CuO_101.6) (Table 8) in order to evaluate the amount of the coating inclusive of phosphate or not, respectively. The free capping agent can be calculated as the difference between the total capping agent amount detected on the not filtered samples and the adsorbed capping agent amount detected on the ultrafiltered ones.

The pristine sample showed the lowest weight loss whilst pristine and modified samples increased the weight loss, due to the presence of the phosphate (used in the buffer solution) and of the capping agents. Likewise the not ultrafiltered samples is higher than the ultrafiltered ones where the capping excess was removed.

Considering the results of ultrafiltered samples inherent to capping agent it is observed that citrate and ascorbate had the lowest value, equal to 1.3% whilst PEI showed the highest value, equal to 5.8%. Medium value (3.2%) was shown by PVP capping agent. Probably, the negative charge of citrate and ascorbate adversely affects the capping properties on negatively charged CuO NPs in buffer phosphate, with the adsorbed capacity % calculated for CIT and ASC of 40 % and 32%, respectively. Medium adsorbed capacity % was estimated for PVP (49 %), characterized by neutral charge. On the other hand, the positive charge of PEI (adsorbed capacity % = 64%) favors its adsorption on negatively charged CuO NPs, due to the presence of phosphate.

The strong influence of the surface charge on the capping agent adsorption is further confirmed by the data found in STOCK nanosuspensions in MilliQ water (not reported here). In this case the adsorbed capacity % calculated for PEI and ASC resulted, respectively, 36% and 61%, demonstrating the better capping performance of ascorbate on positive charged CuO Np. As shown by zeta potential data (Table 8), CuO NPs showed positive zeta potential value when dispersed in water, thus the negative charged ascorbate capping agent was preferentially absorbed on positively charged CuO NPs.

Table 7. Thermogravimetric results achieved for CuO pristine and modified samples (filtered and not filtered).

Sample	Weight loss (%)	Phosphate + Capping agent		Capping Agent	
		Adsorbed Amount (wt %)	Total amount (wt %)	Adsorbed Amount (wt %)	Total amount (wt %)
CuO NP pristine	2.6				
CuO_101.6 (UF)	3.5	5.6			
CuO_101.6 (NO UF)	4.2		9.5		
CuO_102.6_CIT (UF)	4.7	2.2		1.3	
CuO_102.6_CIT (NO UF)	8.0		5.6		4.6
CuO_103.6_PVP (UF)	6.3	4.3		3.2	
CuO_103.6_PVP (NO UF)	10.1		8.8		7.8
CuO 104.6 PEI (UF)	8.6	6.9		5.8	
CuO 104.6 PEI (NO UF)	11.9		10.7		9.7
CuO 105.6 ASC (UF)	4.7	2.2		1.3	
CuO 105.6 ASC (NO UF)	9.2		6.8		5.9

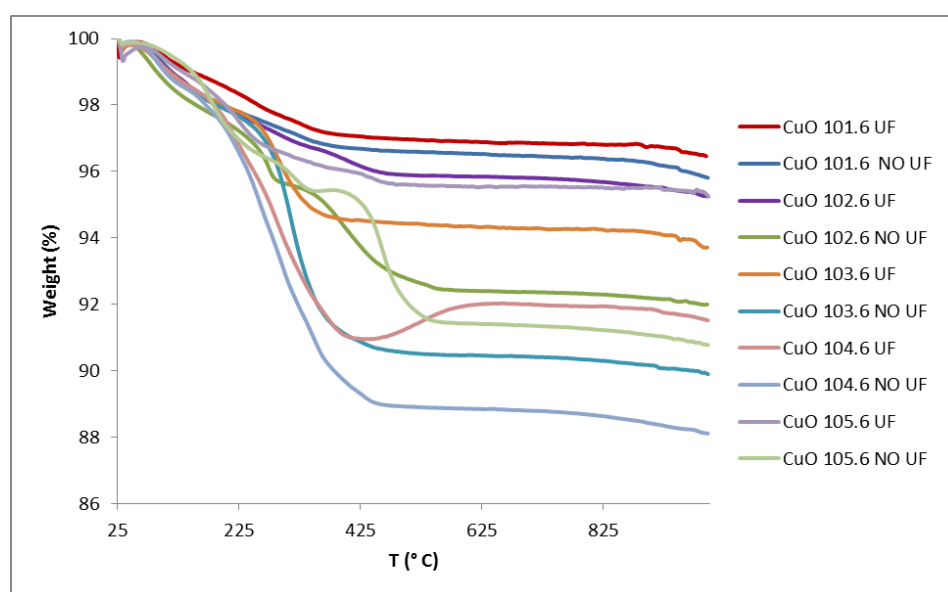


Fig 8. Thermogravimetric curves collected for CuO pristine and modified samples (filtered and not filtered).

Concluding, from thermal analysis results, it is observed that CuO NPs, dispersed in buffer phosphate are coated both by phosphate ions and by the capping agents. Finally, to further confirm the presence of the capping agent (PEI, ASC) adsorbed on the CuO NP surface, the zeta potential measurements were carried out on the powders, obtained after drying of the ultrafiltered suspension then redispersed in water (100 mg/L). The results listed in table 8 evidenced that the ultrafiltered samples, where the capping agent excess was removed, maintained the surface charge typical of the capping agent, so strengthening the assumption of the capping absorption on the NP surface.

Table 8. ζ potential data of CuO samples dispersed in MilliQ water at 100 mg/L.

Sample	Zeta-pot (mV)
CuO 104 PEI UF dispersed in MILLIQ	+41.3 \pm 2.3
CuO 105 Asc UF dispersed in MILLIQ	-14.6 \pm 0.4
CuO_104_PEI_(NO UF)	+28.3 \pm 0.7
CuO_105_ASC_(NO UF)	-17.4 \pm 0.3

2.2.4 – Aging evaluation

pH - In order to evaluate the effect of the aging on the CuO suspensions, a series of characterizations was performed on both fresh and aged samples (after 3 months). The measurements of pH, hydrodynamic diameter and Z-potential were carried out both on stock and working suspensions.

The pH values, measured both on aged and fresh samples, are listed in Table 9.

Table 9 - pH of fresh stock and working suspensions and aged stock and working suspensions, diluted in MILLIQ water.

	pH - FRESH			pH - AGED	
	STOC K	WORKIN G		STOC K	WORKIN G
CuO_101.6_Sol_BM_SYN	9.4	8.3	CuO_101.8_Sol_BM_SYN	9.1	8.2
CuO_102.6_Sol_BM_CIT_S YN	8.7	8.3	CuO_102.8_Sol_BM_CIT_S YN	8.6	8.4
CuO_104.6_Sol_BM_PEI_S YN	10.1	8.8	CuO_104.8_Sol_BM_PEI_S YN	8.4	8.2

CuO_105.6_Sol_BM_ASC_S YN	7.8	7.9	CuO_105.8_Sol_BM_ASC_S YN	7.8	7.8
------------------------------	-----	-----	------------------------------	-----	-----

Despite the presence of phosphate buffer, the stock suspensions showed higher values of pH than the buffer (pH = 7.4). Our hypothesis is that the buffering mechanism is altered both by the interaction of the PO_4^{3-} ions with the CuO surface and by the precipitation of the insoluble copper phosphate $\text{Cu}_3(\text{PO}_4)_2$ salt. The data evidenced very close pH values for both aged and fresh working suspensions, proving the chemical stability of these systems over the storage time. Only the PEI modified sample exhibited a marked pH variation during the storage, probably due to its strong interaction (absorption) with the negative $\text{CuO}/\text{PO}_4^{3-}$ surface.

Particle size distribution – Table 10 shows the average hydrodynamic diameters collected both on fresh and on aged working suspensions (100 mg/l).

Table 10 . Size data (Zeta-average) of fresh samples and aged samples, before and after US treatment.

	d_{DLS} (nm)**		d_{DLS} (nm)	
	FRESH		AGED	AGED – after US
CuO_101.8_Sol_BM_SYN	1093 ± 50	CuO_101.6_Sol_BM_SYN	nd*	1575 ± 188
CuO_102.8_Sol_BM_CIT_SYN	368 ± 10	CuO_102.6_Sol_BM_CIT_SYN	nd*	438 ± 70
CuO_104.8_Sol_BM_PEI_SYN	247 ± 14	CuO_104.6_Sol_BM_PEI_SYN	1207 ± 27	842 ± 57
CuO_105.8_Sol_BM_ASC_SYN	122 ± 1.4	CuO_105.6_Sol_BM_ASC_SYN	nd*	nd*

* nd = not determined *

**Light scattering measurements were made on diluted sample (0.1 mg/ml)

Data collected from fresh samples confirmed the expected effect of the surface modifiers as already observed in the previous section 2.2.1. The 3 months storage produced an increase of the agglomeration degree, clearly observed by the increase of the hydrodynamic diameter even after ultrasonication. In fact, the aged working samples, except for CuO_104_Sol_BM_PEI_SYN, were quite unstable with visible agglomerates. Moreover, in order to allow the DLS measurement and to assess the size distribution of the agglomerates, the ultrasound treatment was applied. The primary particles can form agglomerates by adhesion (weak physical interactions) or aggregates by chemical/sinter forces (metallic, ionic or covalent

bonds). The agglomerates are not fixed units, but could change their size and shape. Altering the characteristics of the surrounding medium (temperature, pressure, pH-value, viscosity, etc.) produced a variation of the agglomerates. Larger agglomerates may break down into smaller ones or, vice versa, smaller agglomerates may again form larger ones. [12].

The data collected after US treatment showed that, except for the ascorbate-modified sample, which during the storage forms compact agglomerates, in the other samples the soft sediment could be easily reduced till values roughly comparable with the fresh samples. PEI, probably due to its strong interaction with the particle surface (as proved by both thermal and ζ potential analyses) seemed to be the dispersant most effective for the long term colloidal stability. On the contrary, the ascorbate was greatly effective on the fresh sample, but not suitable for the long term storage.

ζ Potential - ζ potential data referred to fresh and aged working suspensions are listed in Table 11. As already observed in the previous section 2.2.2, the fresh samples showed values coherent with the charge given by the capping agent. For the pristine and the ascorbate modified sample the aging time leads to a decrease of the colloidal stability, consistent with the DLS data and with the visual observation, and proved by a marked decrease of ζ potential till values close to zero. Therefore positive PEI and negative CIT are the most suitable capping agents for ensuring the over time stability, in fact they preserved high ζ -potential values.

Table 11. ζ potential data of fresh samples and aged samples CuO samples.

Zeta pot _{ELS} (mV) - FRESH		Zeta pot _{ELS} (mV) - AGED	
CuO_101.8_Sol_BM_SYN	-31.3 ± 0.6	CuO_101.6_Sol_BM_SYN	-2.3 ± 0.5
CuO_102.8_Sol_BM_CIT_SYN	-36.5 ± 0.5	CuO_102.6_Sol_BM_CIT_SYN	-35.0 ± 0.6
CuO_104.8_Sol_BM_PEI_SYN	+13.7 ± 0.6	CuO_104.6_Sol_BM_PEI_SYN	+14.7 ± 0.5
CuO_105.8_Sol_BM_ASC_SYN	-35.7 ± 1.5	CuO_105.6_Sol_BM_ASC_SYN	-2.0 ± 1.5

The data are slightly different from data reported in table 6 (MilliQ) because table 6 is referred to partially aged stock solutions (1 month)

2.2.5 – XRD and STEM characterization

In order to verify the effect of the modifiers on the CuO powders in terms of crystalline structure, XRD analyses were performed on both pristine and modified samples. XRD results confirmed the oxide structures for all the analyzed samples, corresponding to the crystalline phase of CuO (JPCDS 65-2309, space group C2/c) and showing that the addition of the different chelating agents did not change the crystalline phase of the material (Fig. 9, 10, 11).

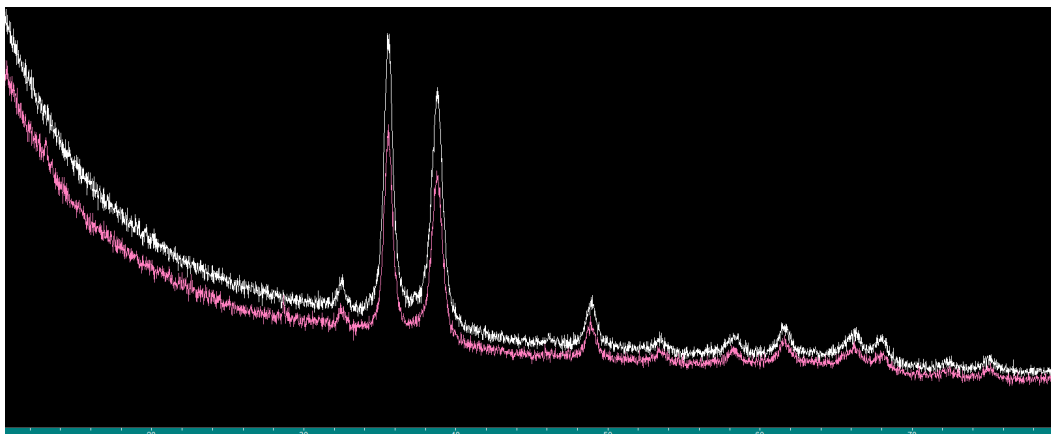


Fig. 9 - XRD pattern of Pristine CuO (pink line) and CuO_{102.8}CIT (white line)

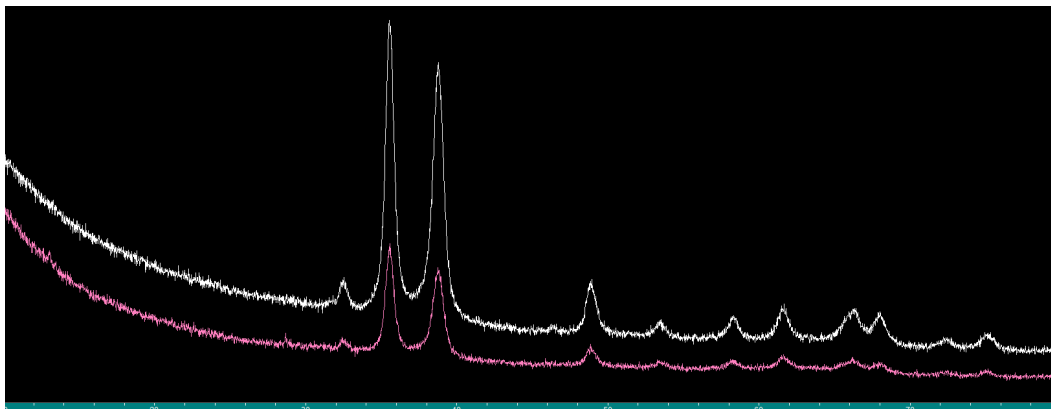


Fig. 10 – XRD pattern of Pristine CuO (pink line) and CuO_{104.8}PEI (white line)

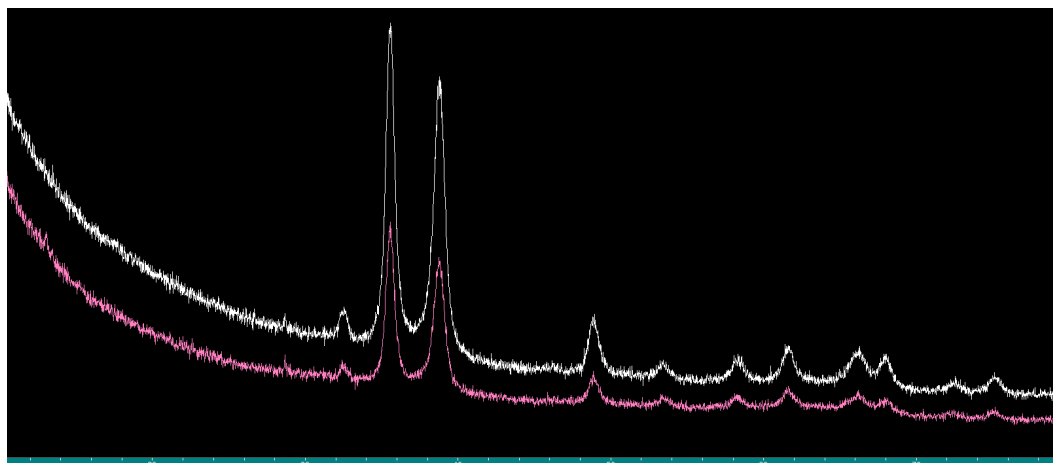


Fig. 11 - XRD pattern of Pristine CuO (pink line) and CuO_105.8_ASC (white line)

The STEM images were performed on samples aged at three months, in particular on CuO pristine powder (Fig 12) and on the ascorbate-modified (Fig 13). The analysis of the images evidenced the presence of primary nanoparticles with an average diameter of about 12 ± 8 nm for the pristine sample and of about 22 ± 9 nm for the ascorbate modified one. As already observed by the hydrodynamic diameters by DLS the aged ascorbate sample resulted more aggregated than the pristine one.

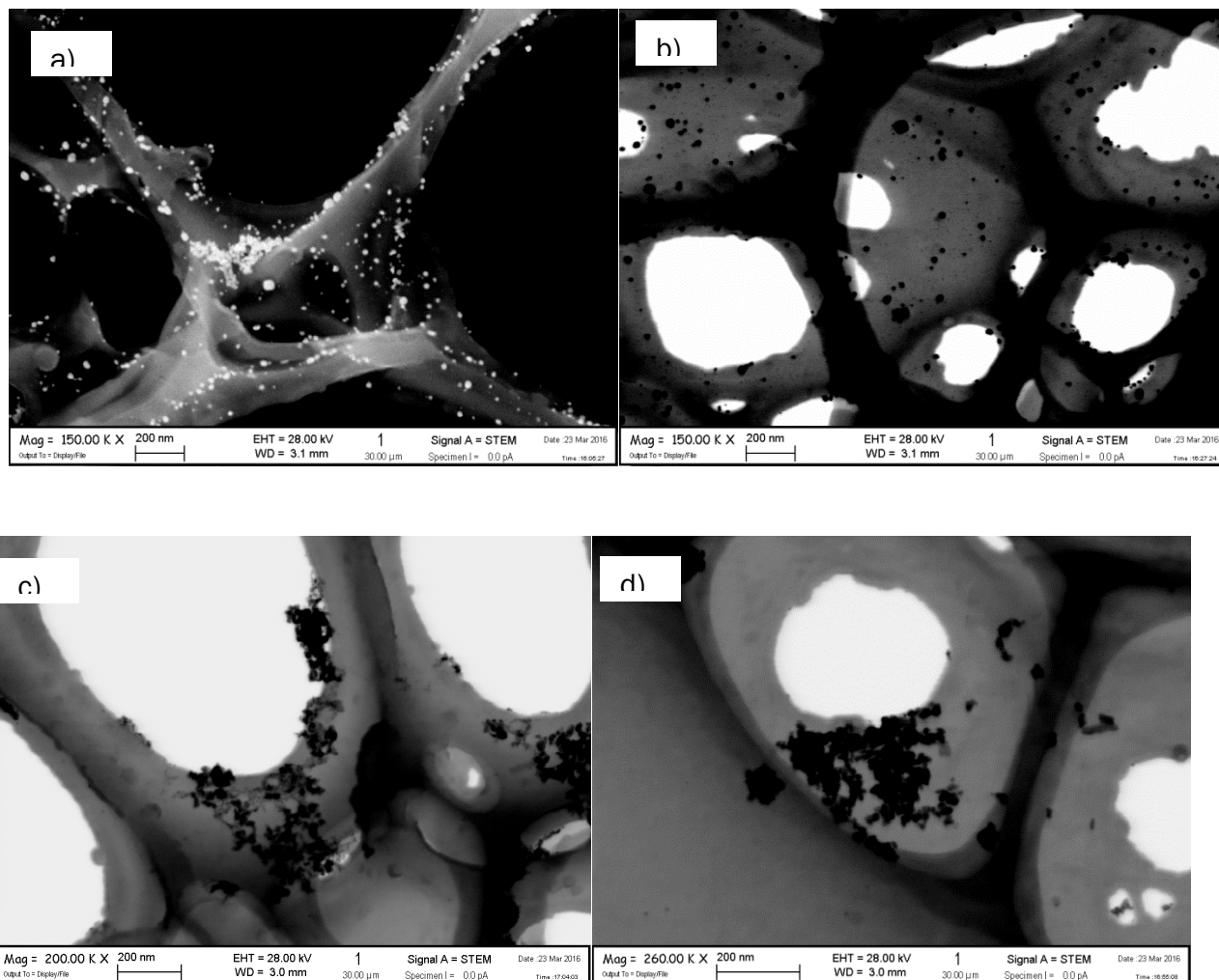


Fig 12 – STEM images of Cu Pristine (a,b) and of Cu_{105.8}_ASC (c,d)

3.0 - Deviations from the workplan

The main important deviation from the workplan was the reversal of the two deliverables deadlines, from:

D7.1 Report on the development of SbyD strategies applied to WC-Co, Month 15

D7.2 Report on the development of SbyD strategies applied to CuO, Month 30

to

D7.1 Report on the development of SbyD strategies applied to CuO, Month 15.

D7.2 Report on the development of SbyD strategies applied to WC-Co, Month 30

4.0 Performance of the partners

The only partners involved with the exception of CNR in Task 7.2 are the partners (MBN NANOMATERIALIA and PLASMACHEM). According to the workplan they provided pristine materials.

5.0 Conclusions

In conclusion WC-Co was modified and characterized as foreseen by the workplan, nine different dispersions were prepared and dried in order to modify the material, finally the optimal dispersion was selected and successfully processed by spray. Even if on the modified materials the dustiness tests are now ongoing at the National Research Centre for the Working Environment, promising data of morphology and of surface area were achieved.

A systematic and not foreseen characterization was performed on CuO in order to better understand the effects of the proposed modifications in eco-tox relevant media. At this purpose a step by step characterization of the modified materials in media with increasing complexity has been performed, monitoring the colloidal properties in terms of stability, hydrodynamic diameter, Z-potential, ion dissolution, aging effect. The results showed that the modifiers markedly changed the colloidal properties according with the charge of the modifiers, then in the biological media the particles are completely covered by the proteins, as expected by the protein corona theory. The ion release assessment showed a strong increase of the dissolution phenomena in the complete biological media, probably due to the chelating power of the aminoacids which subtract the ions from the equilibrium, so promoting dissolution. Concerning the ion dissolution an important activity was performed, and still ongoing, on the development of an electroanalytical tool for the assessment of the in situ ions, avoiding the ultrafiltration and ICP analysis procedures. The data evidenced that the method is suitable for this purpose, detecting ions in the presence of CuO nanoparticles and also in the biological media.

Furthermore the quantification of the organic modifiers was assessed by means of thermal analysis showing the dependence of the coating absorbance from the surface charge, in fact positive coatings are mainly adsorbed in presence of the phosphate buffer, which gives a negative charge to the particle surface. On the other hands negative coatings are mainly adsorbed in water media, where the nanoparticle surface is positive. Finally, the evaluation of the crystalline phase showed that the presence of the modifiers did not modify the crystalline phase, which is always detected as CuO.

In view of these results the present deliverable resulted satisfactory fulfilled.

References

1. N.L. McFarlane, N.J. Wagner, E.W. Kaler, M.L. Lynch, Poly(ethylene oxide) (PEO) and Poly(vinyl pyrrolidone) (PVP) Induce Different Changes in the Colloid Stability of Nanoparticles, *Langmuir* 26 (2010) 13823–13830
2. X. Liu, L. Chen, Aggregation and interactions of chemical mechanical planarization nanoparticles with model biological membranes: role of phosphate adsorption, *Environ. Sci.: Nano* (2015)
3. I. Karimi, B. Hashemi, M. Javidi, S.N. Azadani, Studying effect of various stabilisers on sol electrophoretic deposition of titania, *Surface Eng.* 28 (2012) 737–742
4. T. Xia, M. Kovochich, M. Liong, J.I. Zink, A.E. Nel, Cationic Polystyrene Nanosphere Toxicity Depends on Cell-Specific Endocytic and Mitochondrial Injury Pathways, *ACS Nano* 2 (2007) 85–96.
5. A. Asati, S. Santra, C. Kaittanis, J.M. Perez, Surface-Charge-Dependent Cell Localization and Cytotoxicity of Cerium Oxide Nanoparticles, *ACS Nano* 4 (2010) 5321–5331
6. G.I. Guerrero-García, E. Gonzalez-Tovar, M. Olvera de la Cruz, Effects of the ionic size-asymmetry around a charged nanoparticle: unequal charge neutralization and electrostatic screening, *Soft Matter*, 6 (2010) 2056–2065
7. H.L. Karlsson, P. Cronholm, Y. Hedberg, M. Tornberg, L. De Battice, S. Svedhem, I.O. Wallinder, Cell membrane damage and protein interaction induced by copper containing nanoparticles—Importance of the metal release process, *Toxicology* 313 (2013) 59–69
8. X. Liu, L. Chen, Aggregation and interactions of chemical mechanical planarization nanoparticles with model biological membranes: role of phosphate adsorption, *Environ. Sci.: Nano* (2015)
9. K. Midander, P. Cronholm, H.L. Karlsson, K. Elihn, L. Möller, C. Leygraf, I. Odnevall Wallinder, Surface Characteristics, Copper Release, and Toxicity of Nano- and Micrometer-Sized Copper and Copper(II) Oxide Particles: A Cross-Disciplinary Study, *Small* 5 (2009) 389–399
10. P. Cronholm, H.L. Karlsson, J. Hedberg, T.A. Lowe, L. Winnberg, K. Elihn, I. Odnevall Wallinder, L. Möller, Intracellular Uptake and Toxicity of Ag and CuO Nanoparticles: A Comparison Between Nanoparticles and their Corresponding Metal Ions, *Small* 9 (2013) 970–982
11. Kizic R, Trnkova L, Sevcikova, S, Smarda J, Frantisek J (2002) Silver electrode as a sensor for the determination of zinc in 1141 cell cultivation Medium. *Anal Biochem* 301:8–13
12. M. L. Eggersdorfer et al. *Advanced Powder Technology* 25 (2014) 71–90
13. C. Baldisserrri and A.L. Costa, Electrochemical detection of copper ions leached from CuO nanoparticles in saline buffers and biological media using a gold wire working electrode *Journal of Nanoparticle Research*, 18(4), 1–20, (2016)